European Rotorcraft Forum

# SHIPBOARD LANDING PERIOD BASED ON DYNAMIC ROLLOVER RISK PREDICTION

Binh Dang-Vu
ONERA, France – binh.dangvu@onera.fr

**Abstract**

While SHOLs (Ship/Helicopter Operating Limitations ) provide acceptable wind velocities and orientation and ship motion limits, limited attention has been given to the real-time determination of windows in which ship motions are likely to be safe for helicopter landings and deck handling operations. Existing operational systems developed to indicate periods of quiescence usually combine a specific set of ship motions into a scalar quantity, e.g. an energy index. The contribution of the present paper is to associate forbidden landing windows with the conditions of a control departure when the helicopter landing gear touches the deck of the ship. Among the well-known losses of control, dynamic rollover is particularly critical and hard to recover. A method to determine shipboard landing periods based on dynamic rollover risk prediction is proposed. The objective is to reduce the helicopter hover time and to provide the pilot with a safe go-ahead signal to start the hovering descent to the deck. A simulation tool has been developed, capable of modelling the complex interactions in the dynamic interface between ship and helicopter. Simulation results as well as sensitivity analysis with respect to uncertainties are presented.

## 1. INTRODUCTION

Traditionally, helicopter/ship dynamic interface envelopes have been derived from flight tests at sea. Because of the difficulty in obtaining the proper weather conditions and because safety of helicopter/ship testing is of paramount importance, only a limited number of data points are obtained. The application of piloted flight simulation techniques and analysis tools has long been considered as a complement to sea-trial testing. At ONERA, an offline methodology to determine the Ship/Helicopter Operating Limitations (SHOLs) has been developed recently able to consider both subjective and objective aspects of the ship/helicopter operation [1]. In parallel, another analysis and simulation study has been conducted to determine the time intervals in which a landing can be performed safely. Indeed while the SHOLs provide acceptable wind velocities and orientation and ship motion limits, limited attention has been given to the real-time determination of windows in which ship motions are likely to be safe for helicopter landings and deck handling operations. There exist some operational systems based on real-time measurements of motions which have been developed to indicate periods of quiescence to the pilot or ship operator. These systems are known as Landing Period Indicators (LPI). The methods usually combine a specific set of motions into a scalar quantity, e.g. an energy index, that could efficiently indicate the roughness of the ship motions [2] and additionally include the mechanical and dynamics limits of the helicopter [3, 4, 5]. Simulator and at-sea testing of helicopter recoveries from a common waypoint with and without the LPI have shown a significant reduction of the time to land when the LPI is used.

An alternative approach to determine landing periods is proposed in this paper. It consists of associating forbidden landing windows with the conditions of a control departure when the helicopter landing gear touches the deck of the ship. Among the well-known losses of control, dynamic rollover is particularly critical and hard to recover. As mentioned in Ref. [6], rollover is indeed one of the limiting factors when conducting helicopter/ship qualification testing. Post-landing problems which are more concerned with ensuring the helicopter will not skid, slide, or dynamically tip over after successfully landing are not addressed in this paper. It is assumed that there exist deck restraints or deck-lock systems to secure the helicopter to the deck.

This paper is organized as follows. First, Section 2 recalls briefly the principle that underlies the design and operation of current LPI systems. Section 3 presents an alternative method for determining shipboard landing periods based on the prediction of the risk of rollover. A simulation tool has been developed, capable of modelling the complex interactions in the dynamic interface between ship and helicopter. Section 4 discusses the simulation results as well as the sensitivity analysis of the rollover risk prediction with respect to uncertainties.



Presented at 44th European Rotorcraft Forum, Delft, The Netherlands, 18-20 September, 2018

## 2. LANDING PERIOD INDICATORS FOR HELICOPTER/SHIP OPERATIONS

Current Visual Landing Aids (VLA) for helicopter/ship operations includes flight deck status and signaling systems, hover position indicators and precision approach path indicators. Stabilized glide slope indicator and stabilized horizon bar are visual cues commonly used by the pilot to establish and maintain the proper glide slope, and to start the stationary descent to the deck. LPI systems are complementary VLAs designed to aid the pilot in anticipating ship flight deck quiescent periods that result in acceptable conditions for a shipboard landing. A well-known implementation of LPI concept is the Landing Period Designator (LPD) which has been tested and implemented on ships on a limited scale [4, 5]. The LPD is an electrical/hydraulic/optical device that senses ship acceleration, rate, and displacement motion energy, and presents this energy in terms of a visual landing aid graphical format that pilots can use to help determine when the ship motion is approaching a quiescent or low ship energy condition conducive to a safe landing (Figure 1).

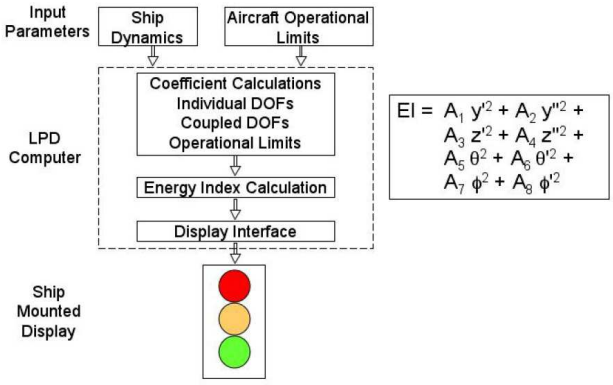


**Figure 1**: LPD operation and Energy Index calculation [5].

The LPD capability to identify the onset of a quiescent period of ship motion is based on the measurement of ship motion and the mechanical and dynamic limits of the helicopter. These limits are expressed as the ship's Energy Index (EI). As indicated in Figure 1, the EI uses eight parameters, roll and pitch, their rates, lateral and vertical velocities and accelerations. All of the parameters are weighted by dynamic coefficients which are weighted according to the individual degree-of-freedom, the coupled degrees of freedom and normalized according to aircraft characteristics. The remaining two degrees of freedom (yaw and surge) are monitored for motion within certain operational limits. The EI is an empirical formulation designed to convert ship motion characteristics and aircraft structural dynamic limits into a meaningful scalar value. It is analogous to the level of kinetic and potential energy contained in the ship. The deck availability is directly based on the ship characteristics, aircraft limitations and pilot-in-the-loop factors (Figure 2).

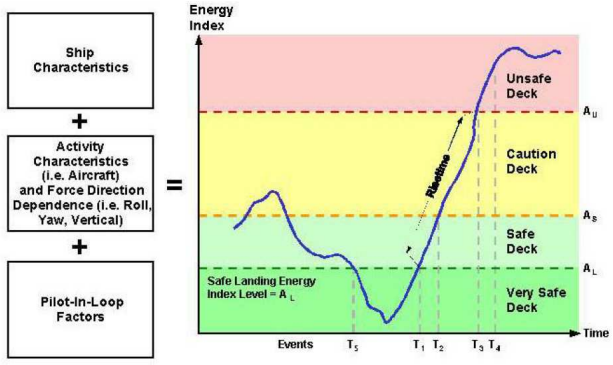


**Figure 2**: Deck availability and rise time [5].

Deck motion safety limits are established for each combination of aircraft and ship and are measured experimentally or calculated analytically. A limit is defined in terms of the impact that a certain ship motion condition may have on the structural integrity or dynamic response of a given helicopter. If the condition exceeds an operational specification, a limit condition is identified. The sum of these limits produces a red line that is drawn on the EI scale for a given ship. The energy defined for a safe deck condition implies that the potential energy being transferred from the sea into the ship's structure is not sufficient to displace the ship into an unsafe deck condition for some specified minimal period of time. This specified minimal period of time required to raise the deck from minimal motion to unacceptable motion is called the rise time (Figure 2) and is dependent on the combination of aircraft and ship. The rise time is the parameter from which the EI visual information is generated.
Simulator and at-sea testing of helicopter recoveries from a common waypoint with and without the LPD have shown a significant reduction of the time to land when the LPD is used.
In the next section a complementary approach to determine landing periods is proposed, based on the prediction of the helicopter roll motion at touchdown. Helicopter pitchback at touchdown is not addressed in this paper.

## 3. DYNAMIC ROLLOVER RISK PREDICTION

Conditions prone to dynamic rollover result generally from an input perturbation in roll while the helicopter is in quasi-hover flight, the rotor lift balancing approximately the weight of the aircraft, one of the two landing gears left or right in contact with the deck creating a pivot around which the tilting takes place. These conditions may be encountered during the



Presented at 44th European Rotorcraft Forum, Delft, The Netherlands, 18-20 September, 2018

final landing phase when the gear in contact with the deck undergoes lateral or vertical acceleration, or when the disturbing roll input is produced by a lateral wind gust. Dynamic rollover results indeed from the displacement of the centre of rotation in roll from the centre of gravity of the helicopter towards the pivot represented by the landing gear in contact with the deck, thus considerably increasing the rolling moment of inertia of the aircraft (in a factor of 6 for a Puma type helicopter) while the rotor control effectiveness remains unchanged.

The behaviour of a helicopter with one of the two main landing gears in contact with the deck of a ship can be modelled as a combination of a number of interacting sub-systems: main rotor, fuselage, tail rotor, landing gear strut, tyre, deck motion. Figure 3 highlights the main moments, forces and accelerations involved in the helicopter roll dynamics model.

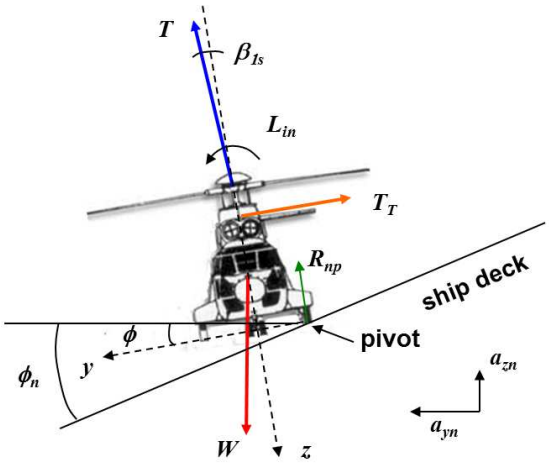


**Figure 3**: Moments, forces and accelerations contributing to helicopter rolling dynamics about the pivot point.

| | |
|---|---|
| $a_{yn}$ | lateral acceleration of ship deck |
| $a_{zn}$ | vertical acceleration of ship deck |
| $L_{in}$ | flapping moment |
| $R_{np}$ | tyre reaction |
| $T$ | main rotor thrust |
| $T_T$ | tail rotor thrust |
| $W$ | helicopter weight |
| $\beta_{1S}$ | rotor lateral flapping angle |
| $\phi$ | helicopter roll angle |
| $\phi_n$ | ship roll angle |

In the proposed concept, the helicopter roll response at touchdown is forecasted while the helicopter is still in the air. This is illustrated by the block diagram of Figure 4. The rollover risk is calculated from the predicted motion of the helicopter and the forecasted motion of the ship deck at touchdown, assuming the pilot actually initiates the go-ahead landing manoeuvre from the hover position above the deck. For instance, initiating a landing from 15ft above the deck with a lift factor equal to 0.9 will lead to touchdown 3 seconds later. After touchdown a full reduction of the collective control is commanded by the pilot model. Any rollover tendency is countered by lowering the collective control and by commanding full opposite cyclic. By updating continuously the calculation of the predicted motions of both the helicopter and the ship deck, the time windows for a safe landing (in the sense of rollover risk) can be determined and presented to the pilot. The level of confidence depends of course on the ability to reliably predict the motions. Current prediction algorithms are able to predict the ship motion satisfactorily for up to 7 seconds.

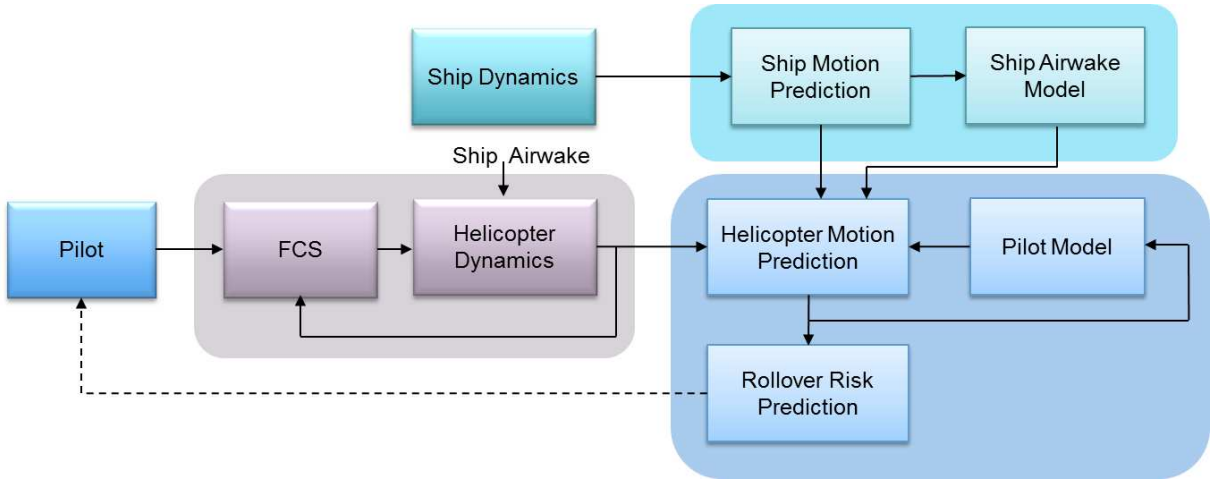


**Figure 4**: Block diagram of rollover risk prediction.



Presented at 44th European Rotorcraft Forum, Delft, The Netherlands, 18-20 September, 2018

A simulation program has been developed to determine shipboard landing periods based on the proposed method. The code is capable of modelling the complex interactions in the dynamic interface between ship and helicopter. As presented in Figure 4, the modules involved in the construction of the dynamic rollover model are the ship motion prediction model, the ship air wake model, the pilot model, the helicopter model while in the air and while in contact with the deck. The analytical modelling of each of the modules is briefly described below.

*Ship motion prediction model*: The motion of a ship is the result of complex hydrodynamic forces between the ship, the water and unknown random processes. There has been extensive research on the modelling of ship dynamics to predict ship motions in response to encountered waves. Statistical prediction methods for the prediction of this motion have been preferred here, to a deterministic analysis which would lead to a ship specific model that involves highly complex calculations [7]. The traditional Auto Regressive and Moving Average ARMA model [8, 9] is used. The method basically finds the best statistical fit to the time history values using time domain coefficients for a stationary process.

Figure 5 shows a recording sequence of the motion of a ship in a sea state 5 over a period of 2 minutes. The time histories plotted are the ship roll angle, lateral acceleration and vertical acceleration (denoted respectively phin, ayn and azn).

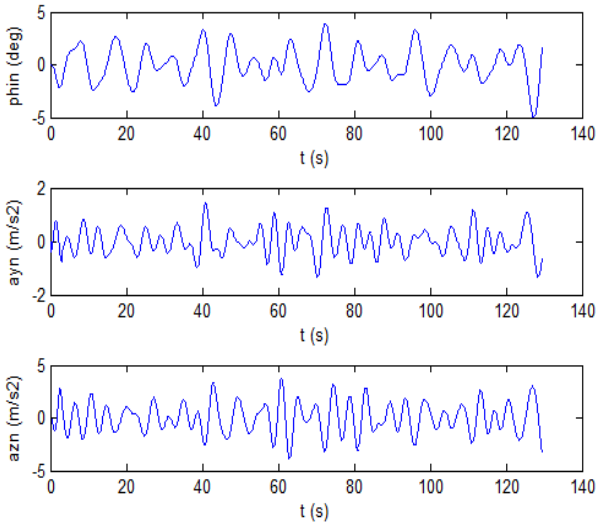


**Figure 5**: Ship motion. Sea state 5.

An ARMA model is fitted to the measured data and predicted motion beyond the estimation data is then calculated. In Figure 6, the past measurements take place from t = 4s to t = 34s and the prediction takes place from t = 34s to t = 38s. In reality this process is performed in real-time continuously.

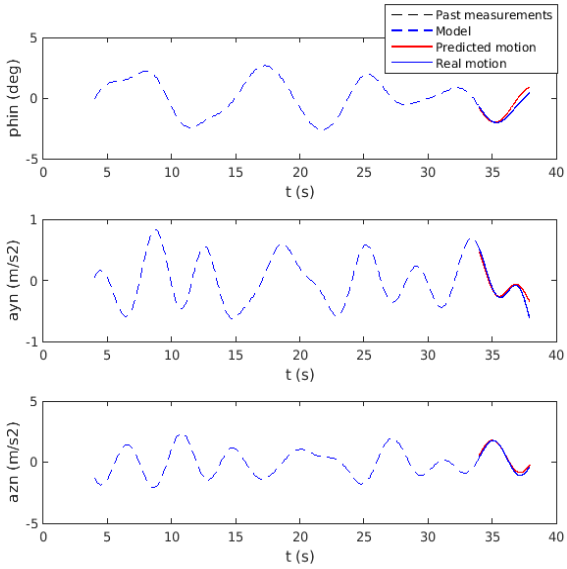


**Figure 6**: Ship motion prediction.

It can be seen that for a prediction interval of 4 seconds, a relatively high accuracy can be obtained. A prediction interval of 4 seconds is actually sufficient because initiating a landing from 15ft above the deck with a lift factor equal to 0.9 will lead to touchdown 3 seconds later. In fact the prediction is continuously calculated over a period ranging from 0 to 8 seconds, i.e. twice the duration of the descent manoeuvre including a pilot reaction time of 1 second. The level of confidence of the rollover risk prediction is directly related to the standard error of ship motion prediction.

*Ship air wake model and helicopter motion prediction model*: The ship air wake model is derived from measurements made on a scaled model frigate in the ONERA-Lille wind tunnel [10]. A simplification of the complex flow field that in reality varies along a rotor blade has been made. The measurements are processed and presented to the helicopter model in terms of the three axis components of wind speed experienced at the rotor hub (Figure 7). The modelling and simulation developed are however believed to be a comprehensive representation of helicopter flight in a ship air wake as test pilots stated that the effect of turbulence on the helicopter were realistic [1]. The helicopter state-space prediction model calculates the behaviour of the helicopter while in the air, assuming the pilot actually initiates the go-ahead landing manoeuvre from the hover position above the deck, as well as the behaviour at and immediately after touchdown from the forecasted motion of the ship deck. The helicopter prediction model is continuously initialized by the real aircraft state variables, the latter are measured or estimated.
The helicopter motion prediction model includes a landing gear model detailed hereafter.



Presented at 44th European Rotorcraft Forum, Delft, The Netherlands, 18-20 September, 2018

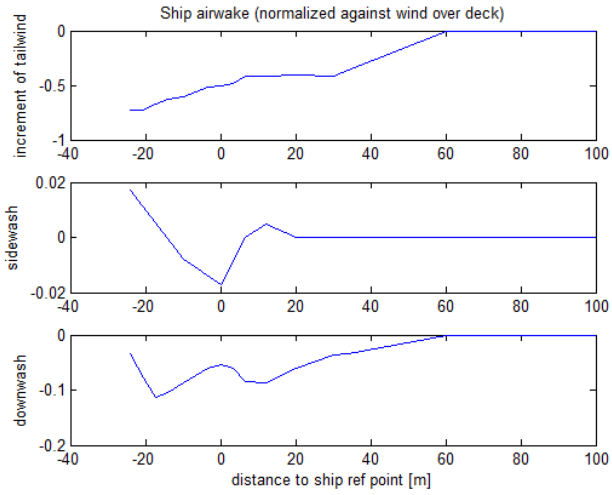


**Figure 7**: Ship airwake [10].

*Landing gear model*: A mathematical model of a main landing gear has been developed with all the relevant physical parameters included. The main landing gear system is simulated as a nonlinear dynamic system with two degrees of freedom: vertical displacement of suspended aircraft mass and vertical displacement of undercarriage mass. The undercarriage model contains static and dynamic components for both struts and tyres (Figure 8).

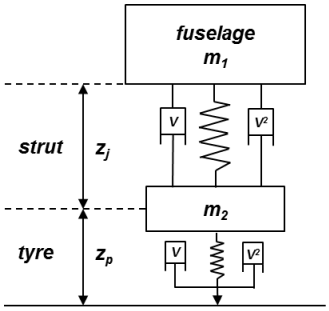


**Figure 8**: Schematic of landing gear model.

The equations for the displacements of the strut and the tyre are:

$$m_1\ddot{z}_j = T - (m_1 + m_2)g + R_{nj} + F_{fj}$$

$$m_2\ddot{z}_p = -m_2 g - R_{nj} - F_{fj} - R_{np} + F_{fp}$$

where

| | |
|---|---|
| $z_j$ | strut length |
| $z_p$ | wheel hub height above deck |
| $R_{nj}$ | strut stiffness |
| $F_{fj}$ | strut friction and hydraulic damping |
| $R_{np}$ | tyre stiffness |
| $F_{fp}$ | tyre damping |
| $T$ | main rotor thrust |

$m_1$ is the equivalent mass of the fuselage excepting the undercarriage.

$m_2$ is the suspended mass (strut and wheel).

The shock strut consists of two series mounted oleo-pneumatic shock absorbers, the low pressure chamber operating for a normal landing and the high pressure chamber absorbing the additional energy when limit landing conditions are exceeded [11]. The stiffness force is calculated analytically as a nonlinear function of oleo extension displacement. These equations contain a pneumatic spring that is determined based on the polytropic gas compression law, a friction that is proportional to the stroke rate, and a hydraulic damping that is proportional to the stroke rate squared. The relation of force to stroke position is,

- compression in the low pressure chamber

$$R_{nj} = = \left( \frac{h_{0BP}}{h_{0BP} - \frac{S}{S_{BP}} c} \right)^{\gamma} p_{0BP} S$$

- compression in the high pressure chamber

$$R_{nj} = \left( \frac{S_{BP} h_{0BP} p_{0BP}^{\frac{1}{\gamma}} + S_{HP} h_{0HP} p_{0HP}^{\frac{1}{\gamma}}}{S_{HP} h_{0HP} + S_{BP} h_{0BP} - Sc} \right)^{\gamma} S$$

| | |
|---|---|
| $c$ | piston displacement |
| $S$ | piston cross sectional area |
| $S_{BP}$ | low pressure chamber sectional area |
| $S_{HP}$ | high pressure chamber sectional area |
| $p_{0BP}$ | low pressure chamber pressure |
| $p_{0HP}$ | high pressure chamber pressure |
| $h_{0BP}$ | low pressure chamber gas height |
| $h_{0HP}$ | high pressure chamber gas height |
| $\gamma$ | adiabatic index of gas |

The parameters of the model have been identified for a Puma type landing gear strut. The evolution of the strut load as a function of strut displacement is shown in Figure 9.

The damping force is calculated as a function of oleo extension displacement, rate of change and direction (compression or rebound):

$$F_{ff} = F_{ff1} + F_{ff2}$$

where

- Friction : $F_{fj1} = -f_1 \dot{z}_j$
- Hydraulic damping : $F_{fj2} = -sign(\dot{z}_j) f_2 \dot{z}_j^2$



Presented at 44th European Rotorcraft Forum, Delft, The Netherlands, 18-20 September, 2018

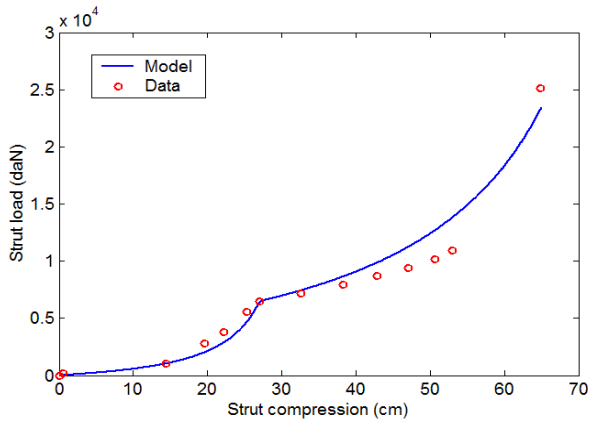


**Figure 9**: Strut load vs. strut compression.

A nonlinear tyre model is added to the strut model. This tyre model has a spring rate that is a function of tyre deflection and damping proportional to compression rate. The vertical reaction of the tyre is calculated analytically by means of a nonlinear function relating the inflation pressure and the actual deflection of the tyre via a polytropic process.

The tyre deformation is a combination of the belt deformation and the flank deformation. To calculate the volume of compressed air, the tyre deformation is approximated by truncating a circle with the radius of the undeformed tyre (Figure 10). The area of the contact patch is given by:

$$S = 2L\sqrt{R^2 - (R-e)^2}$$

and the angle $\theta_e$ delimitating the length of the contact patch is:

$$\theta_e = \cos^{-1}\left(1 - \frac{e}{R}\right)$$

| | |
|---|---|
| $R$ | wheel radius |
| $L$ | tyre width |
| $e = R - z_p$ | tyre deflection (compression) |
| $z_p$ | wheel hub height above deck |

The expression of the tyre reaction is:

$$R_{np} = p_0 \left[ \frac{\left(\pi R^2 - \pi R_j^2\right)}{\left(\pi R^2 - \pi R_j^2 - R^2\left(\theta_e - \cos\theta_e \sin\theta_e\right)\right)} \right]^{\gamma} S$$

| | |
|---|---|
| $R_j$ | rim radius |
| $p_0$ | inflation pressure |
| $\gamma$ | adiabatic index of gas |

Figure 11 shows the load of a 615X225-10 tyre versus the tyre compression for an inflation pressure of 10bars.

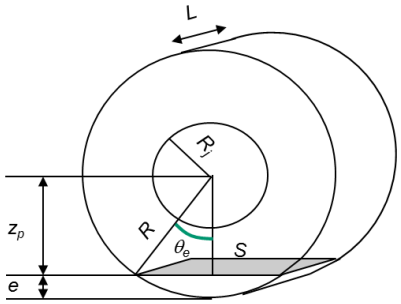


**Figure 10**: Area and length of contact patch.

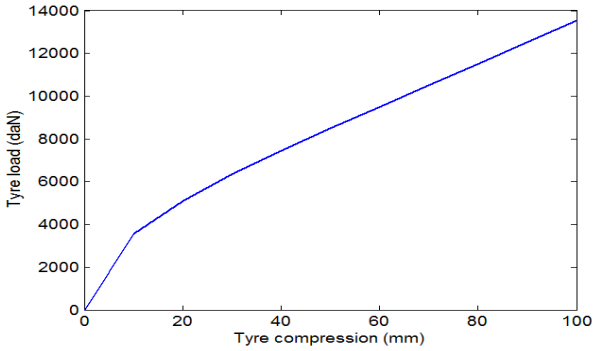


**Figure 11**: Tyre load vs. tyre compression.

At touchdown, the pivot point may be fixed or may slide due to the helicopter motion, the ship motion, and the ship deck surface roughness. It is assumed that the tyre in contact with the deck has either no sideslip or is at pure lateral (or cornering) condition. The contact patch deflection is exclusively in the lateral direction and therefore only a lateral force is generated. A calculation of the sideslip angle at which the tyre reaches full sliding can be found in Ref. [12]. A simpler model is used here. The lateral force developed at the tyre-deck contact patch is related to the normal load via a friction coefficient, which is assumed constant and dependent only on the ship deck surface. This determines the adhesion/sliding limit of the pivot point.

*Pilot model*: The flight segments associated with the shipboard landing are limited to the final approach, hovering above the deck and descent to the deck. A serial model structure with inner and outer loops is retained for the pilot model. The inner-loop pilot function is modelled as a compensatory tracking task to control the helicopter attitude. The outer-loop pilot function is modelled as a guidance strategy to control the helicopter position. The go-ahead landing from hover is initiated by applying a slight reduction to the lift factor, a common value being 10%. After touchdown a full reduction of the collective control is commanded by the pilot model. Any rollover tendency is countered by lowering the collective control and by commanding full opposite cyclic [13].



Presented at 44th European Rotorcraft Forum, Delft, The Netherlands, 18-20 September, 2018

## 4. SIMULATION RESULTS

### 4.1. Critical rollover angle

A steady-state analysis is first conducted in order to determine the critical rollover angle according to the most sensitive parameters.
Figure 12 shows, for a Puma type aircraft, the critical rollover angle as a function of the helicopter thrust to weight ratio and the ship deck lateral acceleration. The gear in contact with the deck is the left gear. This is the most unfavourable of the two possible main landing gear contact configurations for this helicopter because the tail rotor thrust acts in the direction of rolling (see Figure 3). The commanded rotor lateral flapping angle $\beta_{1s}$ to counter the rollover is assumed fixed and equal to -5deg. For a given thrust to weight ratio, any roll attitude below the boundary leads to a rollover departure. As shown in Figure 12, the absolute value of the critical rollover angle increases as the thrust to weight ratio decreases. It is well-known that the appropriate action to counter rollover tendency is to lower the collective control. The lateral acceleration of the ship deck is an important parameter contributing to dynamic rollover. The absolute value of the critical rollover angle decreases as the deck lateral acceleration increases.

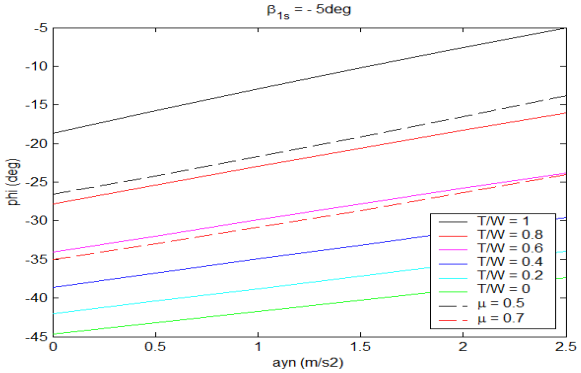


**Figure 12**: Helicopter critical rollover angle vs. thrust to weight ratio and lateral acceleration of ship deck.

The dotted lines in Figure 12 are the roll angle boundaries below which the pivot point slides on the ship deck. The boundaries for two friction coefficients of the deck surface are plotted, corresponding to a wet deck ($\mu$=0.5) and a dry deck ($\mu$=0.7). For helicopter roll angles at touchdown below the sliding boundary and above the rollover boundary, the pivot point will slide reducing the rollover risk.
Figure 13 shows, for a thrust to weight ratio equal to 0.9, the critical rollover angle as a function of the deck lateral acceleration and the helicopter roll control capability represented by the margin to maximum deflection of the lateral flapping angle $\beta_{1s}$. The roll control capability at landing may be dramatically reduced if a large part is already used to counter a strong side wind on the deck. For a given margin of lateral flapping angle $\beta_{1s}$, any helicopter roll attitude below the boundary leads to a rollover departure. It can be seen that the absolute value of the critical rollover angle decreases as the roll control capability decreases. It also decreases as the deck lateral acceleration increases. Current operational limits correspond to a lateral acceleration of the order of 1.5 m/s$^2$. For a roll control margin of $\beta_{1s}$ = -5deg and for a thrust to weight ratio equal to 0.9, a rollover departure will occur if the helicopter roll angle exceeds 16 deg. The dotted lines represent the roll angle boundaries below which the pivot point slides on the ship deck.

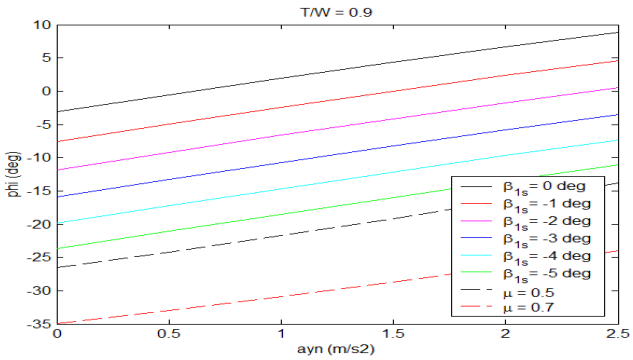


**Figure 13**: Helicopter critical rollover angle vs. lateral acceleration of ship deck and roll control capability.

Figure 14 shows the critical rollover angle as a function of the lateral and vertical accelerations of the deck. The thrust to weight ratio is equal to 0.9 and the rolling control capability corresponds to a lateral flapping angle of -5 deg. A descending vertical acceleration of the deck increases the risk of rollover as long as a pivot point exists i.e. the landing gear tyre remains in contact with the deck.

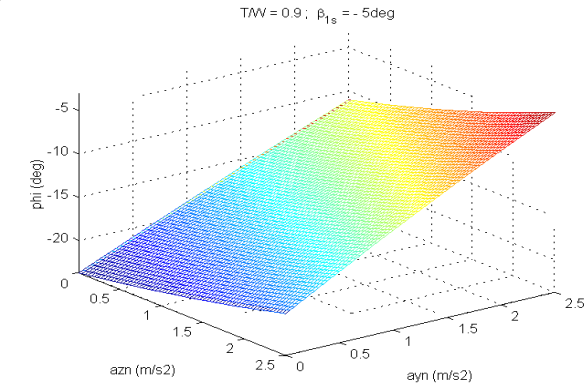


**Figure 14**: Helicopter critical rollover angle vs. lateral and vertical accelerations of ship deck.



Presented at 44th European Rotorcraft Forum, Delft, The Netherlands, 18-20 September, 2018

### 4.2. Approach phase and descent from stationary hover point

Simulations are performed for approaches, hovering over the deck and landing for a Puma type helicopter. The landing manoeuvre is assumed to begin with the helicopter keeping station with ship from an astern position. The ship is travelling at 10kt, in 10kt headwind, and with the helicopter positioned at a distance of 200ft and height 15ft above the landing point (Figure 15).

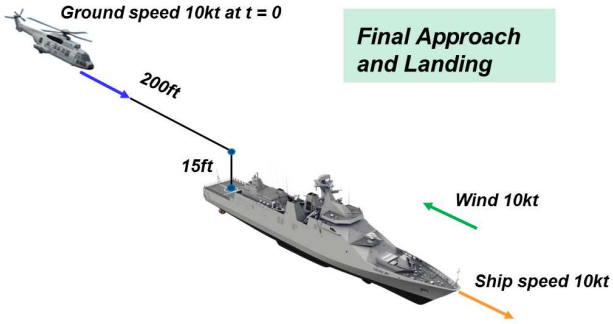


**Figure 15**: Final approach and landing.

The time histories of a simulated landing are plotted in Figure 16. The variables are roll, pitch, yaw and their rates, position with respect to the landing point, ground speed components (uk0,vk0,wk0), airspeed components (u,v,w) in aircraft body-axes. Heading and glide slope angles are denoted khi and gamma.
The first phase of the manoeuvre is a forward step to a position over the deck where a period of time is taken to stabilize the helicopter and to wait for a slot for a safe landing. The outer-loop pilot function is modelled as a guidance strategy to control the helicopter position. The inner-loop pilot function is modelled as a compensatory tracking task to control the helicopter attitude. The dotted lines in the phi, theta, psi plots represent the inner-loop pilot control orders in roll, pitch and yaw. The manoeuvre starts with a quick pitch-down command in order to increase ground speed from 10kt to 20kt followed by a pitch-up control order to reduce ground speed to 10kt to keep station with ship above the landing point. The effects of ship airwake are countered by control inputs in roll, pitch, yaw and heave.
The second phase of the landing manoeuvre is the vertical descent onto the deck and touchdown. This phase is not initiated until a safe landing slot has been identified. As shown in Figure 16, the descent begins at time t = 30s and touchdown is 3.32s later. The helicopter vertical speed at touchdown is -0.5 m/s and roll angle is 2deg. A zoom-in view of the helicopter motion after touchdown is discussed in the next section. In fact a large number of touchdown cases will be simulated to determine the helicopter response as a function of the touchdown instant. By varying the instant of deck contact from the current instant, the landing periods can be determined.

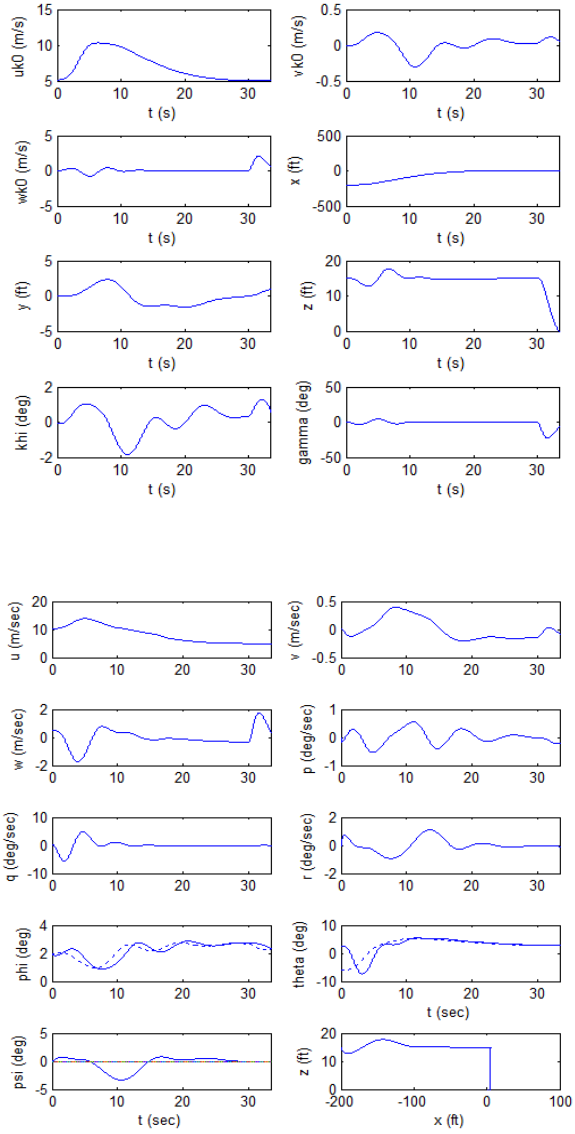


**Figure 16**: Approach phase and descent from stationary hover point.

### 4.3. Determination of landing periods

The final descent onto the deck is not initiated until a safe landing slot has been identified. For this, the rollover risk is calculated from the predicted motion of the helicopter and the forecasted motion of the ship deck at touchdown, assuming the pilot actually initiates the go-ahead landing manoeuvre from the hover position above the deck. Below are two examples of landing periods determination based on two ship motion sequences recorded at sea.

*Sequence 1*: Figure 17 presents a recording sequence of the motion of a ship in a sea state 5 over a period of 2 minutes. The plotted variables are the ship deck roll angle, pitch angle, vertical velocity, lateral and vertical accelerations. The predicted helicopter types of responses after touchdown at



Presented at 44th European Rotorcraft Forum, Delft, The Netherlands, 18-20 September, 2018

each instant of the time histories are calculated and identified on the plots as follows. Time intervals plotted in green correspond to helicopter roll transients less than 10deg and no pilot action in the roll axis. Time intervals plotted in red correspond to a recovered rollover with roll transients exceeding 10deg. Time intervals plotted in orange correspond to a vertical speed exceedance according to MIL-S-8698 specifications [14]. The landing periods are therefore represented by the green time intervals, assuming a perfect prediction of the ship motion.

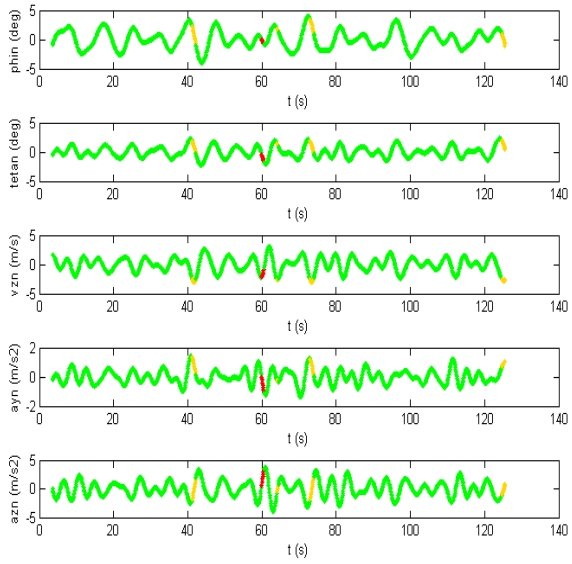


**Figure 17**: Sequence 1 time histories of ship deck motion with rollover tendencies.

A good prediction of the ship motion can be obtained up to 4 seconds while the duration of the descent phase from hover at 15ft over the deck to touchdown is about 3 seconds. The descent onto the deck can be initiated inside a green time interval at least 4 seconds before it ends. This allows a pilot reaction time of 1 second. In fact the prediction is extended to a longer time horizon, of the order of 7, 8 seconds to avoid initiating a descent manoeuvre that ends outside a green time interval. A display symbology for a safe go-ahead signal to start the hovering descent to the deck could consist of a coloured light similar to a traffic light. The light is green if the first 4 seconds of prediction and the following 4 seconds of prediction are inside a green time interval. The light is yellow if the first 4 seconds of prediction only are inside a green time interval. The light is red for all the other cases.
Figure 18 shows the zoom-in view of the time histories of Figure 17 between time t = 45s and time t = 75s. A rollover departure with roll transient exceeding 10deg is predicted around t = 60s. A simulation is run to show the helicopter response after touchdown.

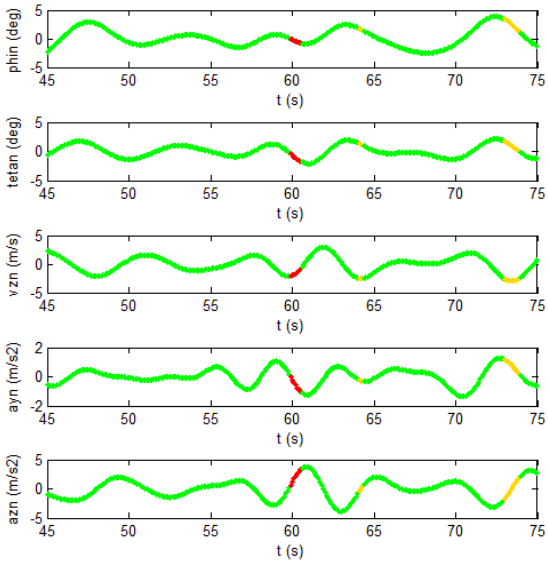


**Figure 18**: Time interval [45s; 75s] of Sequence 1.

The contact with the deck occurs at time t = 60.30s, roll angle of the ship is phin = -0.56deg, lateral acceleration is ayn = -0.75 m/s2, vertical acceleration is azn = 2.58m/s2. Helicopter initial roll angle is phi = 0 deg. Therefore it is the right landing gear that first comes into contact with the deck. Helicopter vertical speed at touchdown is -0.5m/s and ship vertical speed is 1.42m/s. The helicopter lift to weight ratio is 0.9 at touchdown. The helicopter response after touchdown is presented in Figure 19 where t = 0 is the touchdown instant. A lift reduction of the main rotor and the rear rotor (denoted respectively T and Tt) is observed following the reduction of the collective pitch 0.5 seconds after the contact of the right landing gear with the deck. The motion of the helicopter after touchdown is a rollover departure about the right landing gear. As the roll angle reaches 10deg, a full opposite cyclic is commanded by the pilot model at t = 1.28s. The rollover departure is stopped following the combined action of collective reduction and opposite cyclic. The left gear touches the deck at time t = 2.28s. Once the two main landing gears are in contact with the deck, the time evolution of the helicopter roll angle is the same as the ship roll angle. As post-landing roll angle is below the steady-state critical rollover boundary (Figure 12), the two main landing gears remain on the deck. Figure 19 shows also the time histories of the strut piston travel, the tyre deflection, the strut stiffness and tyre stiffness of both landing gears. The tyre of the right landing gear around which the roll motion takes place remains in contact with the deck.
The effect of a dispersion of the helicopter roll angle at touchdown will be discussed in Section 4.4.



Presented at 44th European Rotorcraft Forum, Delft, The Netherlands, 18-20 September, 2018

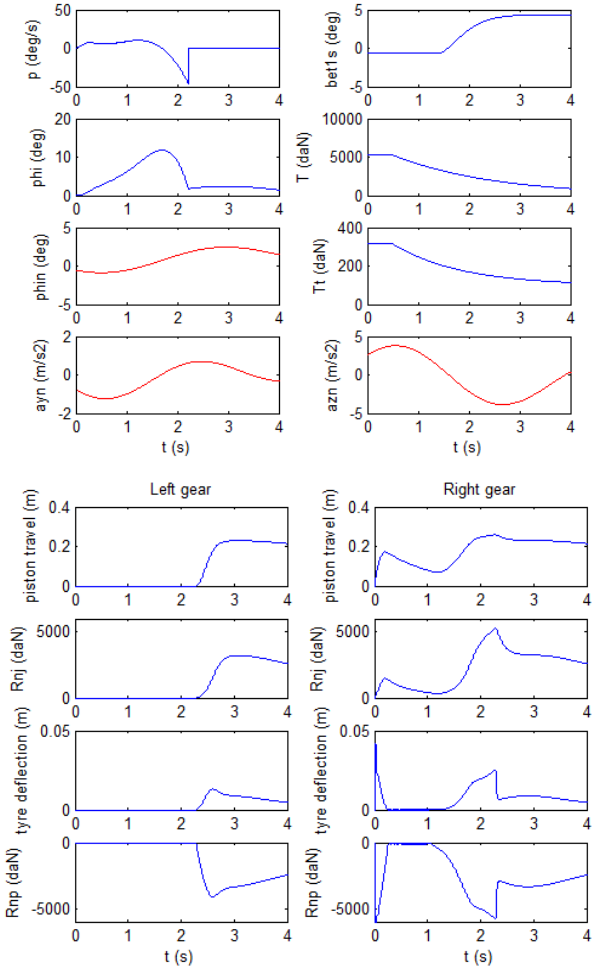


**Figure 19**: Helicopter motion after touchdown.

*Sequence 2*: Figure 20 presents another recording sequence of the motion of a ship in a sea state 5 over a period of 2 minutes. The plotted variables are the ship deck roll angle, pitch angle, vertical velocity, lateral and vertical accelerations. The predicted helicopter types of responses after touchdown at each instant of the time histories are identified as follows. Time intervals plotted in green correspond to helicopter roll transients less than 10deg and no pilot action in the roll axis. Time intervals plotted in red correspond to a recovered rollover with roll transients exceeding 10deg. Time intervals plotted in black correspond to an unrecovered rollover. Time intervals plotted in orange correspond to a vertical speed exceedance. Time intervals plotted in magenta correspond to a ship pitch angle exceedance. The landing periods are therefore represented by the green time intervals, assuming a perfect prediction of the ship motion. As discussed above, a safe go-ahead signal to start the hovering descent to the deck could consist of a coloured light similar to a traffic light. The light is green if the first 4 seconds of prediction and the following 4 seconds of prediction are inside a green time interval.

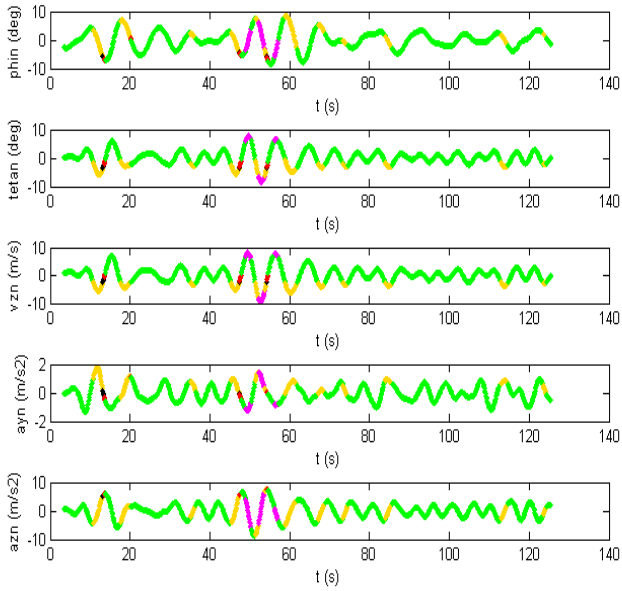


**Figure 20**: Sequence 2 time histories of ship deck motion with rollover tendencies.

Figure 21 shows the zoom-in view of the time histories of Figure 20 between time t = 5s and time t = 35s. A rollover occurrence is predicted around t = 13s.

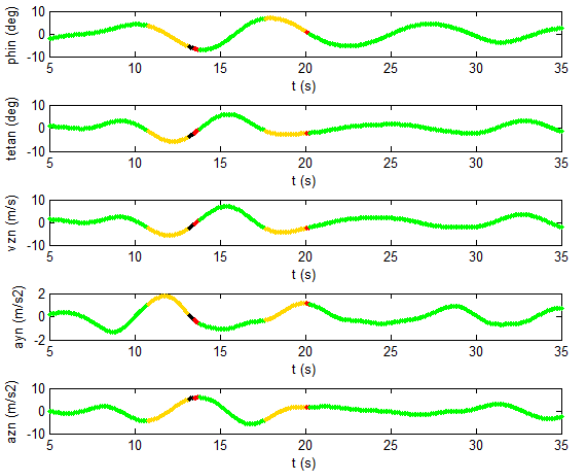


**Figure 21**: Time interval [5s; 35s] of Sequence 2.

A simulation is run to show the helicopter response after touchdown leading to an unrecovered rollover. The contact with the deck occurs at time t = 13.31s, ship roll angle is -6.05 deg, lateral acceleration is ayn = -0.02m/s2 and vertical acceleration is azn = 5.47m/s2. The helicopter roll angle at touchdown is 0 deg. Therefore it is the right gear that first comes into contact with the deck. Helicopter vertical speed at touchdown is -0.5m/s and ship



Presented at 44th European Rotorcraft Forum, Delft, The Netherlands, 18-20 September, 2018

vertical speed is -1.82m/s. Helicopter lift to weight ratio at touchdown is 0.9. The helicopter response after touchdown is presented in Figure 22. A rollover departure is countered by the pilot from time t = 1.31s when the roll angle reaches 10 deg. However the rollover cannot be recovered and the rotor blades tips touch the deck at time t = 1.75 s.

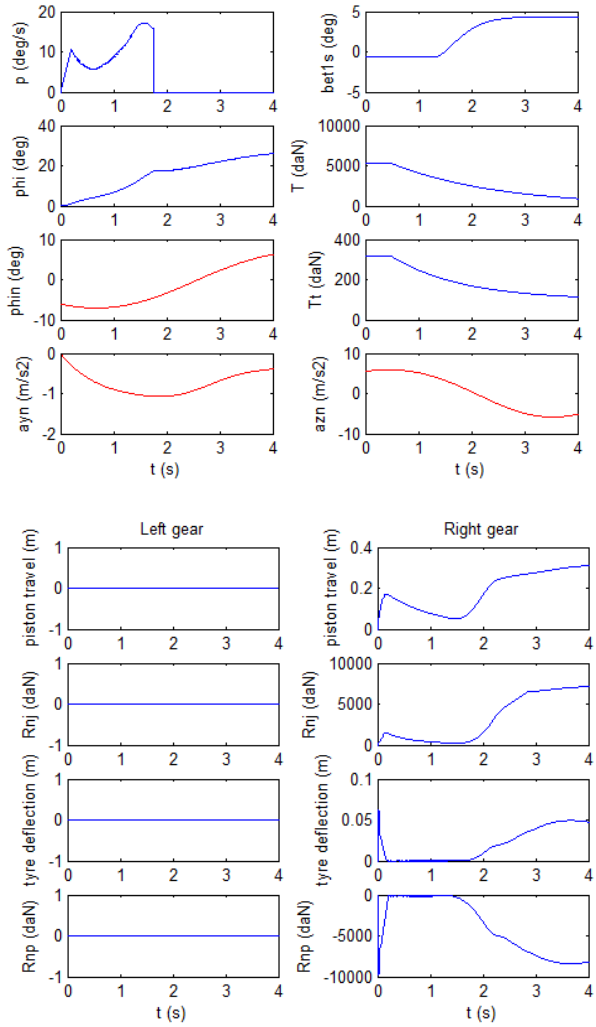


**Figure 22**: Helicopter motion after touchdown.

The rollover is due to a descending vertical acceleration of the deck while the tyre of the right landing gear around which the roll motion takes place still remains in contact with the deck.

### 4.4. Sensitivity analysis

Statistic results on rollover risk with respect to uncertainties are presented below. Differences between the real motions of helicopter and ship and their predicted motions lead to errors in the prediction of the rollover risk. Monte Carlo simulations are run to analyse the impact of influential parameters on the level of confidence with which the landing period can be validated. The sensitivities investigated include the dispersions concerning the helicopter roll angle at touchdown and the prediction accuracy of ship lateral acceleration.

Sensitivity with respect to helicopter roll angle at touchdown is presented in Figure 23. The Monte Carlo simulations are performed as follows. A random safe landing case is chosen inside a green time interval of the sequence shown in Figure 17 (or Figure 20). For a given standard deviation of the roll angle, a number of 100 simulations are performed and for each one the rollover tendency is determined. The standard deviation of the helicopter roll angle is increased up to and beyond a value for which a rollover departure is observed. The process is repeated for 100 random safe landing cases chosen in the sequence. The distribution function in Figure 23 indicates the percentage of simulations for which helicopter roll transients are less than 10deg (green plot), the percentage for which a rollover with roll transients exceeding 10deg is successfully recovered (red plot), and the percentage for which an unrecovered rollover occurs (black plot).

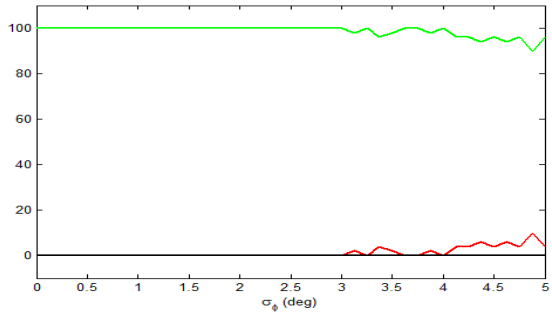


**Figure 23**: Sensitivity to helicopter roll angle standard deviation at touchdown.

The distribution function indicates that helicopter roll angle standard deviation should not exceed 3deg from the model which is used for prediction. Assuming 1D normal distribution, a high level of confidence is thus maintained if helicopter roll angle deviations are less than 9deg.

Sensitivity with respect to ship lateral acceleration is shown in Figure 24. The distribution function indicates that ship lateral acceleration standard error should not exceed 0.25m/s2 from the ARMA model used to predict ship motion.

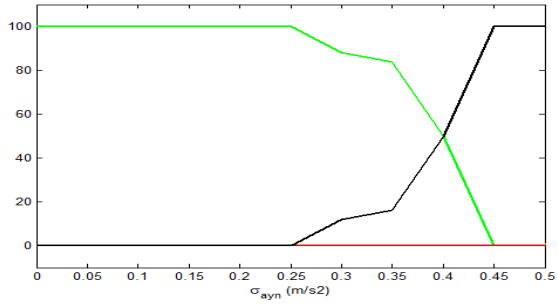


**Figure 24**: Sensitivity to ship lateral acceleration standard error at touchdown.



Presented at 44th European Rotorcraft Forum, Delft, The Netherlands, 18-20 September, 2018

## 5. CONCLUSION

Existing operational systems developed to indicate periods of quiescence usually combine a specific set of ship motions into a scalar quantity, e.g. an energy index. The contribution of the present paper is to associate forbidden landing windows with the conditions of a control departure when the helicopter landing gear touches the deck of the ship. Among the well-known losses of control, dynamic rollover is particularly critical and hard to recover. A method to determine shipboard landing periods based on dynamic rollover risk prediction is proposed. The objective is to reduce the helicopter hover time and to provide the pilot with a safe go-ahead signal to start the hovering descent to the deck. Helicopter pitckback at touchdown is not addressed in this paper. However the ship pitch attitude and vertical speed are monitored for motion within certain operational limits.

A simulation tool has been developed, capable of modelling the complex interactions in the dynamic interface between ship and helicopter. Simulation results as well as sensitivity analysis with respect to uncertainties are presented.

A display symbology for a safe go-ahead signal to start the hovering descent to the deck could consist of a coloured light similar to a traffic light. The light is green if the first 4 seconds of prediction and the following 4 seconds of prediction are inside a green time interval for which helicopter roll transients at touchdown are less than 10deg. The light is yellow if the first 4 seconds of prediction only are inside a green time interval. The light is red for all the other cases. To keep a high level of confidence in the prediction system, helicopter roll angle standard deviation at touchdown should not exceed 3deg from the model used for prediction. Ship lateral acceleration standard error should not exceed 0.25m/s2 from the ARMA model used to predict ship motion. The proposed concept will be further evaluated through piloted simulations.

## REFERENCES

1. Figueira, J.M.P., Taghizad, A., and Abid, M., “The Use of Simulation Tools to Estimate Ship-Helicopter Operating Limitations”, AIAA Modeling and Simulation Technologies Conference, Denver, Colorado, USA, June 5-9, 2017.

2. O'Reilly, P.J.F., “Aircraft/Deck Interface Dynamics for Destroyers”, Marine Technology, Vol. 24, No. 1, Jan. 1987, pp. 15-25.

3. Ferrier, B., Polvi, H., and Thibodeau, F.A., “Helicopter/Ship Analytic Dynamic Interface”, AGARD CP-509, Aircraft Ship Operations, 1991.

4. Ferrier, B., and Manning, T., "Simulation and Testing of the Landing Period Designator (LPD) Helicopter Recovery Aid", Naval Engineers Journal 110 (1): 189-205, 1998.

5. Carico, G.D., and Ferrier, B., “Evaluating Landing Aids to Support Helicopter/Ship Testing and Operations”, IEEE 0-7803-9546-8/06, 2006.

6. Carico, G.D., et al., “Helicopter/Ship Qualification Testing”, RTO-AG-300 Vol. 22, 2003.

7. Price, W.G., and Bishop, R.E.D., “Probabilistic Theory of Ship Dynamics”, Chapman and Hall Ltd, 1974.

8. Box, G.E.P., and Jenkins, G.M., “Time Series Analysis: Forecasting and Control”, Holden-Day, 1976.

9. Box, G.E.P., Jenkins, G.M., and Reinsel, G.C. “Time Series Analysis: Forecasting and Control (Third ed.)”, Prentice-Hall, ISBN 0130607746, 1994.

10. Taghizad, A., Verbeke, Ch., and Desopper, A., “Aerodynamic Perturbations on the Frigate La Fayette Deck - Effects on the Helicopter Flight Dynamics”, Paper C-15, 20th ERF, Rome, 1999.

11. Lopez, C., “Méthode d’optimisation des trains d’atterrissage d’hélicoptère”, Thèse NNT 2007ENAM0038, Arts et Métiers ParisTech, 2007.

12. Kiébré, R., “Contribution to the Modelling of Aircraft Tyre-Road Interaction”, PhD Thesis NNT 2010MULH4086, Université de Haute Alsace, Mulhouse, 2010.

13. Advisory Circular AC 90-87, Helicopter Dynamic Rollover, Federal Aviation Administration, 1986.

14. Military Specification Structural Design Requirements, Helicopters (MIL-S-8698), July, 1954.

## COPYRIGHT STATEMENT





Presented at 44th European Rotorcraft Forum, Delft, The Netherlands, 18-20 September, 2018